PHYSICAL REVIEW B VOLUME 49, NUMBER 4 15 JANUARY 1994-II

Rapid Communications

Rapid Communications are intended for the accelerated publication of important new results and are therefore given priority treatment both in the editorial office and in production. A Rapid Communication in **Physical Review B** *should be no longer than four printed pages and must be accompanied by an abstract. Page proofs are sent to authors.*

Microwave dielectric response of mesoscopic metallic regions and the intrinsic metallic state of polyaniline

J. Joo, Z. Oblakowski, and G. Du
Department of Physics, The Ohio State University, Columbus, Ohio 43210-1106

J. P. Pouget
Laboratoire de Physique des Solides, Université Paris–Sud, 91405 Orsay, France

E. J. Oh,* J. M. Wiesinger, Y. Min, and A. G. MacDiarmid
Department of Chemistry, University of Pennsylvania, Philadelphia, Pennsylvania 19104

A. J. Epstein
Department of Physics and Department of Chemistry, The Ohio State University, Columbus, Ohio 43210-1106
(Received 20 October 1993)

We report the dependence of the microwave-frequency dielectric constant and dc conductivity on the crystallinity and local order of doped polyaniline. The dramatic increase of the dielectric response in the three highest crystalline physically crosslinked polyaniline samples provides evidence for the formation of three-dimensional coupled mesoscopic metallic regions. We report the measurement of a negative dielectric constant in polyaniline (doped with camphor sulfonic acid) demonstrating the intrinsic metallic nature of polyaniline.

Efforts have been made to define the intrinsic metallic state of conducting polymers since their discovery in the late 1970s. Evidence of the intrinsic metallic state can be detected from the temperature (T) independent Pauli susceptibility,[1] thermopower[2] proportional to T, and the negative temperature coefficient of conductivity.[3] Considerable controversy exists concerning the one-[4,5] or three-dimensional[6,7] (3D) nature of this metallic state. As 1D models cannot account for the stabilization of metallic states against the Peierls instability,[8] 3D approaches emphasizing interchain interaction have emerged from both theory[9] and experiment.[7] Further, there exists controversy concerning application of quasi-1D variable-range-hopping models[7] or granular metallic models[6,10] to charge transport of the system. The dielectric response is important for understanding not only the intrinsic metallic nature but also charge localization and its temperature dependence. In this paper we report that at low T, the dielectric constant (ϵ) is proportional to the square of the crystalline domain coherence length determined by x-ray diffraction (ξ^2) for both parallel and perpendicular directions, establishing that the metallic state of polyaniline is three dimensional. At high T, ϵ increases modestly for poorly coupled metallic regions. It increases dramatically for well-coupled regions forming 3D coupled mesoscopic[11] metallic regions, which can be considered as the beginning of the macroscopic metallic state. Samples of polyaniline with camphor sulforic acid (CSA) as counter ion and processed with m-cresol solvent have a negative dielectric constant demonstrating achievement of a delocalized metallic state for specific structural conditions.

The synthesis of XPAN-ES (Ref. 12) and PAN-CSA (m-cresol) (Refs. 13 and 14), where PAN is polyanaline, XPAN is crosslinked polyanaline, and ES is emeraldine salts has previously been reported. Four classes of physically crosslinked (XPAN-ES), one conventional emeraldine hydrochloride salt form of polyaniline (PAN-ES) and polyaniline doped with CSA in $CHCl_3$ and m-cresol solutions [PAN-CSA (m-cresol)] were used for this study, Table I. The experimental techniques for x-ray

TABLE I. X-ray coherence length ξ and effective delocalization length L_{RT} determined from ϵ_{mw}. Note that $\xi_{\perp}^{a}$, $\xi_{\perp}^{b}$, and $\xi_{\parallel}$ are obtained from $\Delta'(2\theta)$ of (200), (010), and (002) ES-II reflections, respectively. Also, i, h, and n refer to intermediate, high, and noncrosslinked samples, respectively. The stretch ratio (l/l_0) is given in parentheses (e.g., 3.5×).

Materials	ξ (Å) $\xi_{\parallel}$	$\xi_{\perp}^{b}$	$\xi_{\perp}^{a}$	L_{RT} (Å) $\parallel$	$\perp$
A^i: XPAN-ES[a] (3.5×)	73	57	29	1200	350
B^h: XPAN-ES[a] (3.5×)	64	47	23	1200	330
C^h: XPAN-ES[b] (5.5×)	57	45	21	880	300
D: PAN-ES[b] (4×)	52	42	23	300	120
E^n: XPAN-ES[b] (1×)		~15		210	

[a]High molecular weight samples.
[b]Low molecular weight samples.

(σ_{dc}),[7] and microwave-frequency measurement[7,16] have been presented previously. The microwave dielectric constants (ϵ_{mw}) at room temperature (RT) dramatically increase from ~800 for the lowest crystalline XPAN-ES to $\sim 3.3\times10^4$ for the highest crystalline XPAN-ES with an exponential temperature (T) dependence of ϵ_{mw}. The slope of $\log_{10}[\sigma_{dc}(T)]$ vs $T^{-1/2}$ for the highest crystalline XPAN-ES, $T_0(K)$, is much less (~700 K) than that of the lowest crystalline XPAN-ES (~3800 K), which implies that the polymer chains between metallic islands are better ordered in the higher crystalline materials. Therefore, the increase in size of the metallic islands (observed in x-ray and low-temperature ϵ_{mw} experiments) and of the degree of order for chains between those islands [obtained from $\sigma_{dc}(T)$] enables the formation of 3D coupled "mesoscopic" metallic regions. The T-dependent microwave conductivity σ_{mw} of PAN-CSA (m-cresol) increases with decreasing T, from RT to ~200 K ($\equiv T_c$), which implies the dominance of the intrinsic metallic behavior. There is a weak-localization behavior in σ_{mw} below T_c. A negative and increasing ϵ_{mw} (from RT to T_c) proves the intrinsic metallic nature of this polymer. In contrast PAN-CSA ($CHCl_3$) is more disordered and behaves similarly to less crystalline XPAN-ES. Hence the fraction of crystallinity and coherence within the crystalline and disordered regions, not counter ion, control the metallic state.

X-ray studies provide information about the percent crystallinity, crystalline domain size, and local order in the crystalline and amorphous regions. The Scherrer equation,[15] $\xi=0.9\lambda/[\cos\theta_0\Delta'(2\theta)]$, where λ (=1.542 Å) is the wavelength of the source, θ_0 is the Bragg angle, and $\Delta'(2\theta)$ is the full width at half maximum of the crystalline diffraction peak, was applied to estimate the size of the crystalline domains, ξ, for both parallel (||) and perpendicular ($\perp$) directions, Table I. Values range from $\xi=15$ Å for the quasiamorphous sample E to 73 Å for $\xi_{\|}$ of sample A having about 50% crystallinity. Compared to sample C, sample D exhibits a lower percent of crystallinity and a greater paracrystalline broadening of the diffraction peaks due to cumulative disorder within the crystalline regions. Though each of samples $A-D$ have the ES-II structure, sample E has ES-I local order.[15]

Below 50 K, ϵ_{mw} of each sample asymptotically approaches a unique value $\epsilon_{mw}(T\to0)$ which is proportional to each sample's ξ^2, Fig. 1. We estimate the localization length L using $\epsilon_{mw}(T\to0)=\epsilon_0+(2^{9/2}/\pi^3)e^2N(E_F)L^2$, where ϵ_0 is from core polarization and e is the electron charge.[7] Assuming $L\sim\xi$, the plot of $\epsilon_{mw}(T\to0)$ vs ξ^2, Fig. 1, yields $N(E_F)\sim1.23$ states/(eV 2 rings). This value is close to that obtained from magnetic studies.[1,7,17,18] *The proportionality of* $\epsilon_{\|}\propto\xi_{\|}^2$ *and* $\epsilon_{\perp}\propto\xi_{\perp}^2$ *with the same proportionality constant demonstrates the 3D nature of the metallic state in XPAN-ES.* The fact $\xi\sim L$ represents that as $T\to0$ the metallic island size is directly related to the crystalline coherence length.

Despite the universality of the $\epsilon_{mw}(T\to0)\propto\xi^2$ behavior, the T dependence of σ_{dc} and ϵ_{mw} varies. The σ_{dc} for all the hydrochloride salts $A-E$ decreases with decreasing T, Fig. 2. The quasi-1D variable-range-hopping (VRH) model,[7,19] $\sigma(T)\propto\exp[-(T_0/T)^{1/2}]$, where $T_0=16/k_BN(E_F)L_{\|}L_{\perp}^2$, $N(E_F)$ the density of states at the Fermi level and $L_{\|(\perp)}$ the localization length in parallel (perpendicular) direction, respectively, provides the best fit to the data through the entire T range for $D(\|)$ and E samples only, with $T_0=4300$ and 3800 K, respectively. We label these samples type II. T_0, the effective energy separation between localized states, is a measure of the degree of disorder in amorphous regions. For $T\le\sim100$ K, T_0 values are 700, 900, and 1000 K for samples A (||), B (||), and C (||), respectively (type-I materials). The lower T_0 implies that polymer chains of type-I materials are more coherently organized in the less-ordered regions than those of type-II materials in accordance with the x-ray-diffraction results. Localized charges in the metallic islands can be more easily delocalized through the more ordered (rodlike) chains as T in-

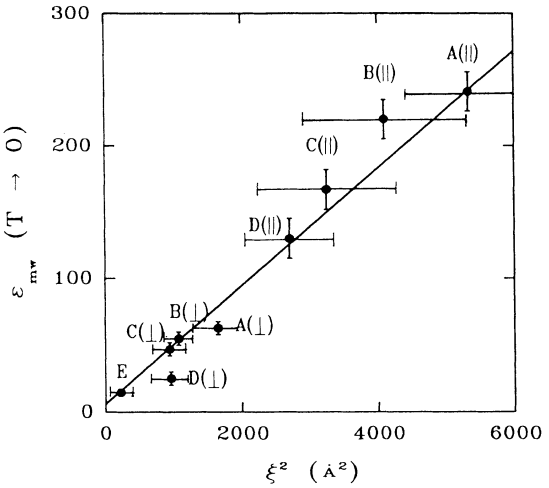

FIG. 1. $\epsilon_{mw}(T\to0)$ vs ξ^2 for XPAN-ES ($\xi_1^2\equiv\xi_1^{(a)}\times\xi_1^{(b)}$).

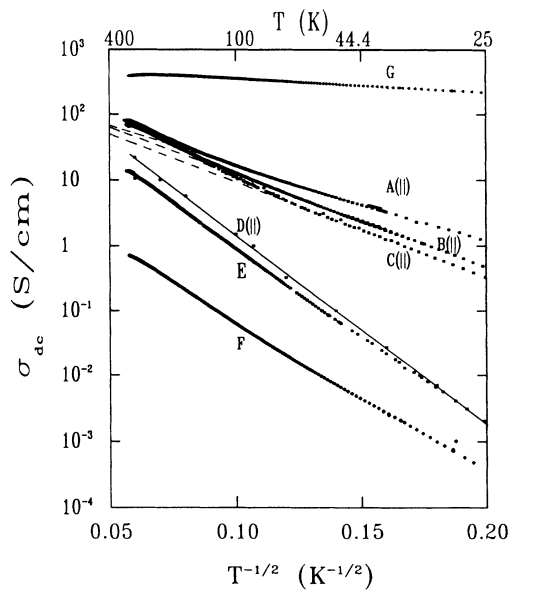

FIG. 2. $\sigma_{dc}(T)$ for XPAN-ES samples. Data for D (||) are from Ref. 7. The dotted straight lines for A (||), B, (||), and C (||) are based upon the quasi-1D VRH model. σ_{dc} for PAN-CSA prepared in $CHCl_3$ (F) and m-cresol (G) are also shown.

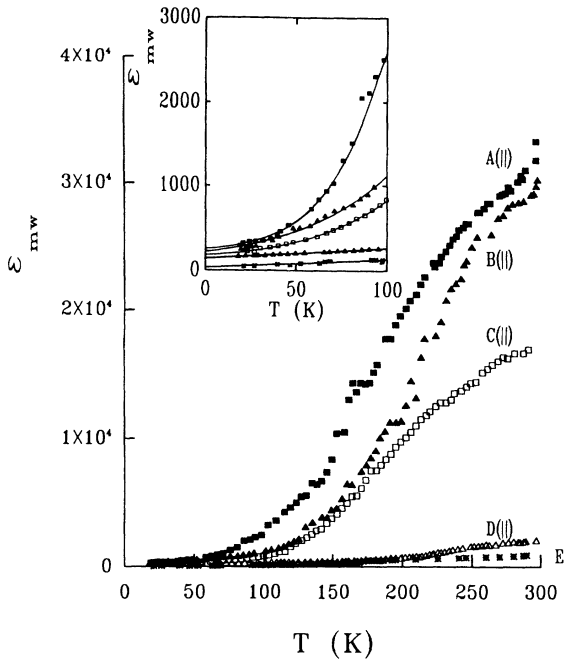

FIG. 3. The comparison of $\epsilon_{mw}(T)$ of XPAN-ES. Inset: A magnified version of the figure below 100 K.

creases, possibly extending through several islands. This may account for the deviation of $\sigma_{dc}(T)$ from the quasi-1D VRH model above ~ 100 K in type-I materials.

The low-T (≤ 100 K) data of XPAN-ES for ϵ_{mw}, inset Fig. 3, shows $\epsilon_{mw} \propto T^2$ behavior in type-I materials and $\epsilon_{mw} \propto T$ for type-II samples. In this regime, because the charge motion is confined to the vicinity of isolated metallic islands and the energy is insufficient to overcome the disordered potential barriers between metallic islands, the interrupted metallic strands (IMS) model[20] is suggested to account for the data. The low-frequency IMS limit $\epsilon_{mw} \simeq 1+\lambda\omega_p^2\tau_r^2$ where $\lambda \rightarrow 1$ at low T and τ_r is the relaxation time with insulating defects, predicts the $\epsilon_{mw} \propto T$ and $\epsilon_{mw} \propto T^2$ behaviors for the relatively small and large proportional constant κ, respectively [assuming $\tau_r \propto \xi + \Delta L(T)$ with $\Delta L(T) \equiv \kappa T$]. At high T (≥ 100 K), the exponential increase of $\epsilon_{mw}(T)$ in type-I materials can be interpreted by the considering more than one hop at a finite frequency with a small T_0.[21] In type-II samples, the $\epsilon_{mw}(T)$ ($T \geq 100$ K) has a power-law behavior due to the relative large T_0. Table I also includes the effective room-temperature delocalization length L_{RT} obtained using ϵ_{mw}(RT). For the type-I materials at RT charges delocalize over $\sim 4-8$ crystalline regions for parallel and perpendicular directions while for lower crystallinity type-II materials charges remain confined to the vicinity of one or two metallic islands. Hence, for type-I materials, 3D coupled mesoscopic metallic regions form with increasing T.

Though the granular-metal model (GMM) also predicts $\sigma_{dc} \propto \exp[-(T_0/T)^{1/2}]$, it is not appropriate for these samples. The anisotropies, $\sigma_{\parallel}/\sigma_{\perp}$ and $\epsilon_{\parallel(mw)}/\epsilon_{\perp(mw)}$ of the samples $A-D$ are ≥ 5 and ≥ 10, respectively; GMM does not account for this anisotropy. Also T-dependent thermoelectric power and electric-field-dependent conductivity studies of these samples yield quantitative analysis within the quasi-1D VRH model and are inconsistent with the prediction of GMM.[22]

Recently, there has been an effect to promote crystallinity by using secondary dopants, such as m-cresol, in PAN-CSA.[13,14,17] Rehgu reported[3] the intrinsic metallic nature of PAN-CSA (m-cresol) based upon the positive T coefficient of resistivity in the range from 180 to 300 K. While $\epsilon_{mw}(T)$ and $\sigma_{mw}(T)$ for PAN-CSA prepared in $CHCl_3$ are similar to those of samples D and E discussed above, the behavior of m-cresol prepared PAN-CSA is dramatically different, Fig. 4. We contrast $\sigma_{dc}(T)$ of PAN-CSA (m-cresol) with that obtained for the same polymer/counterion in chloroform, PAN-CSA ($CHCl_3$) in Fig. 2 (samples G and F, respectively). The difference in behavior (metallic vs localization) is attributed to solvent (m-cresol) -induced structural order in the m-cresol prepared material. The sample prepared in m-cresol has $\sim 50\%$ crystallinity with ES-I-like chain array, and coherence lengths $\xi_{\parallel} \sim 50$ Å and $\xi_{\perp} \sim 30$ Å. It is noted that for ES-I structure adjacent chains are in phase while they are out of phase for ES-II,[15] therefore, electrons may be more readily delocalized in the direction for the most efficient perpendicular transport in the ES-I system. In contrast, the $CHCl_3$ prepared sample is less crystalline with similar structure and coherence lengths to sample G but with increased disorder within the crystalline regions. The $\sigma_{mw}(T)$ increases from RT to T_c, then decreases from ~ 700 S/cm at T_c to ~ 180 S/cm at 4.2 K, inset Fig. 4, similar to $\sigma_{dc}(T)$. The dielectric constant of PAN-CSA (m-cresol) is *negative* from RT to 4.2 K.[16] From the

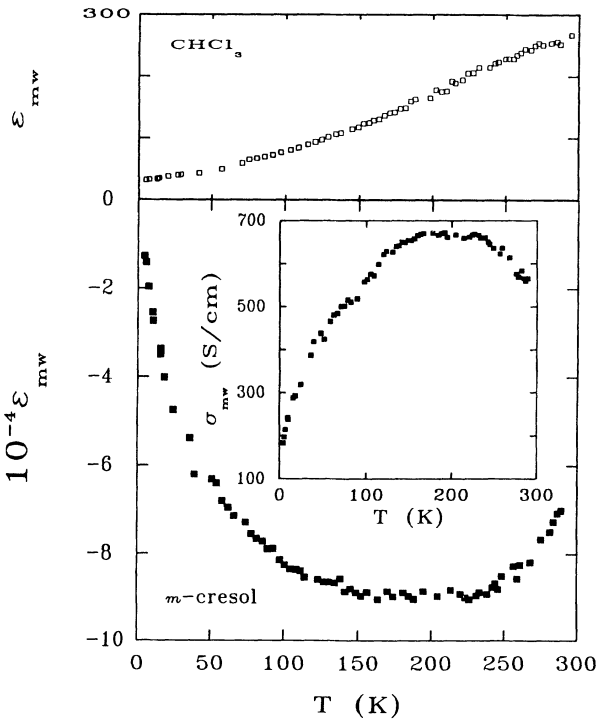

FIG. 4. $\epsilon_{mw}(T)$ of PAN-CSA prepared in $CHCl_3$ and m-cresol. Inset: $\sigma_{mw}(T)$ of PAN-CSA (m-cresol).

Drude model at low frequency ($\omega\tau \ll 1$), the dielectric constant and conductivity are described as $\epsilon \simeq -\omega_p^2\tau^2$ and $\sigma \simeq (\omega_p^2/4\pi)\tau$, respectively, where ω_p is the plasma frequency and τ is the scattering time.[23] The increase in τ as T is reduced to T_c is caused by the diminished effect of thermal phonons. Below T_c, the effects of localization become stronger, and the delocalization length (which is proportional to τ) decreases. We estimate the plasma frequency $\omega_p \sim 0.015$ eV using the relation $\omega_p \sim 4\pi\sigma_{mw}/\sqrt{-\epsilon_{mw}}$. τ is estimated to be $\sim 1.2\times 10^{-11}$ sec at RT. This anomalous long τ may originate from the phonon backscattering rather than from the forward scattering. The key to the appearance of intrinsic metallic $\sigma_{dc}(T)$, $\sigma_{mw}(T)$, and $\epsilon_{mw}(T)$ is the coupling of mesoscopic (crystalline) 3D metallic regions through relatively coherent disordered polymer.

We conclude that the range of charge delocalization is structurally controlled by the fraction of crystalline material, and local order in the crystalline and amorphous regions. The enlargement of metallic islands and the 3D coupling through the more rodlike[12,14] chains between metallic islands induces the 3D coupled mesoscopic metallic regions in XPAN-ES. The increase of crystallinity induced by the conformational changes from coil-like in PAN-CSA ($CHCl_3$) to more rodlike in PAN-CSA (*m*-cresol) contributes to the transition to an intrinsic metallic nature which is confirmed by the negative T coefficient of σ_{mw} and the negative ϵ_{mw}.

We thank V. Prigodin for useful discussions and A. Burns for assistance. This work was partially supported by ONR Grant No. N00014-92-J1369, NSF INT. Grant No. 9016586, and Action Incitative CNRS-NSF. The Laboratorie de Physique des Solides is "Unite Associée au Centre National de la Recherche Scientifique."

*Present address: Dept. of Chemistry, Myong Ji University, Korea.

[1] J. M. Ginder, A. F. Richter, A. G. MacDiarmid, and A. J. Epstein, Solid State Commun. **63**, 97 (1987).

[2] A. B. Kaiser, Phys. Rev. B **40**, 2806 (1989).

[3] M. Reghu, Y. Cao, D. Moses, and A. J. Heeger, Phys. Rev. B **47**, 1758 (1993).

[4] K. Mizoguchi, M. Nechtschein, J. P. Travers, and C. Menardo, Phys. Rev. Lett. **63**, 66 (1989).

[5] P. Phillips and H. L. Wu, Science **252**, 1805 (1991).

[6] F. Zuo, A. Angelopoulos, A. G. MacDiarmid, and A. J. Epstein, Phys. Rev. B **36**, 3475 (1987).

[7] Z. H. Wang, C. Li, E. M. Scherr, A. G. MacDiarmid, and A. J. Epstein, Phys. Rev. Lett. **66**, 1745 (1991); Z. H. Wang, E. M. Scherr, A. G. MacDiarmid, and A. J. Epstein, Phys. Rev. B **45**, 4190 (1992). In this last reference, $\epsilon_{mw}(T) \propto T^2$ for sample D ($\|$).

[8] S. A. Kivelson and A. J. Heeger, Phys. Rev. Lett. **55**, 308 (1985); E. M. Conwell, H. A. Mizes, and S. Jevadev, Phys. Rev. B **40**, 1630 (1989).

[9] S. A. Kievelson and M. Salkola (unpublished).

[10] Q. Li, L. Cruz, and P. Phillips, Phys. Rev. B **47**, 1840 (1993).

[11] *Transport Phenomena in Mesoscopic Systems,* edited by H. Fukuyama and T. Ando (Springer-Verlag, New York, 1992). Based on this reference, we use "mesoscopic" to represent charge delocalization on the scale of ~ 1000 Å.

[12] A.G. MacDiarmid, Y. Min, J. M. Wiesinger, E. J. Oh, E. M. Scherr, and A. J. Epstein, Synth. Met. **55**, 753 (1993).

[13] Y. Cao, P. Smith, and A. J. Heeger, Synth. Met. **48**, 91 (1992).

[14] A. G. MacDiarmid, J. M. Wiesinger, and A. J. Epstein, Bull. Am. Phys. Soc. **38**, 311 (1993); A. J. Epstein, J. Joo, C. Y. Wu, A. Benatar, C. F. Faisst, Jr., J. Zegarski, and A. G. MacDiarmid, in *Proceedings of the NATO Advanced Research Workshop on Applications of Intrinsically Conducting Polymers, Burlington, 1992,* edited by M. Aldissi (Kluwer, Dodrecht, 1993), p. 165.

[15] J. P. Pouget, M. E. Jozefowicz, A. J. Epstein, X. Tang, and A. G. MacDiarmid, Macromolecules **24**, 779 (1991).

[16] In the microwave cavity perturbation method, the depolarization factor (α) was prudently chosen based upon $\sigma_{dc}(T)$ and the room temperature ϵ_{mw} and σ_{mw} obtained by the microwave impedance bridge technique (8.2–12.4 GHz). The change of ϵ_{mw} and σ_{mw} varying with α for XPAN-ES is $\pm 5\%$ for a significant change in α. However, for the PAN-CSA (*m*-cresol) case, a 1% change of α induces a 30% change of the final results. To assure accuracy a Nb thin film coated on glass was used as a reference for metallic samples. The temperature-dependent raw data of PAN-CSA (*m*-cresol) are similar to that of the Nb sample.

[17] Y. Cao and A. J. Heeger, Synth. Met. **52**, 193 (1992).

[18] Our value for $N(E_F)$ is based upon 293 Å^3 for unit volume in Ref. 14. The previous value of $N(E_F)$ obtained from magnetic studies was 1.6 states/eV 2 rings. When the unit volume, 425 Å^3 in Ref. 3, is used, $N(E_F) \sim 1.8$ states/eV 2 rings.

[19] N. F. Mott and E. Davis, *Electronic Processes Non-crystalline Materials* (Claredon, Oxford, 1979).

[20] M. J. Rice and J. Bernasconi, J. Phys. F **2**, 905 (1972).

[21] E. P. Nakhmedov, V. N. Prigodin, and A. N. Samukhin, Fiz. Tverd. Tela (Leningrad) **31**, 31 (1989) [Sov. Phys. Solid State **31**, 368 (1989)].

[22] J. Joo *et al.* (unpublished).

[23] G. Burns, *Solid State Physics* (Academic, New York, 1985).